Radiology

ORIGINAL RESEARCH • GASTROINTESTINAL IMAGING

# Multicenter Validation of Abbreviated MRI for Detecting Early-Stage Hepatocellular Carcinoma

*Takeshi Yokoo, MD, PhD • Nobuaki Masaki, BA • Neehar D. Parikh, MD, MS • Barton F. Lane, MD • Ziding Feng, PhD • Mishal Mendiratta-Lala, MD • Chee Hwee Lee, MD • Gaurav Khatri, MD • Tracey L. Marsh, PhD • Kirti Shetty, MD • Colin T. Dunn, MD • Taim Al-Jarrah, BSc • Anum Aslam, MD • Matthew S. Davenport, MD • Purva Gopal, MD • Nicole E. Rich, MD • Anna S. Lok, MD • Amit G. Singal, MD, MS*

From the Departments of Radiology (T.Y., G.K.), Internal Medicine (C.T.D., N.E.R., A.G.S.), and Pathology (P.G.), UT Southwestern Medical Center, 5959 Harry Hines Blvd, POB 1, Ste 420, Dallas, TX 75390-8887; Department of Biostatistics, University of Washington, Seattle, Wash (N.M.); Departments of Internal Medicine (N.D.P., T.A.J., A.S.L.) and Radiology (M.M.L., A.A., M.S.D.), University of Michigan Medical School, Ann Arbor, Mich; Departments of Diagnostic Radiology (B.F.L., C.H.L.) and Internal Medicine (K.S.), University of Maryland, Baltimore, Md; and Division of Public Health Sciences, Fred Hutch Cancer Center, Seattle, Wash (Z.F., T.L.M.). Received April 15, 2022; revision requested May 23; revision received November 12; accepted November 23. **Address correspondence to** T.Y. (email: *takeshi.yokoo@utsouthwestern.edu*).

Supported by the National Institutes of Health (grants U01 CA230694, U01 U01CA230669, U01 CA230690, and U24CA230144).

Conflicts of interest are listed at the end of this article.

See also the editorial by Kim in this issue.

**Radiology 2023; 307(2):e220917 • https://doi.org/10.1148/radiol.220917 • Content codes: GI MR**

***Background:*** Abbreviated MRI is a proposed paradigm shift for hepatocellular carcinoma (HCC) surveillance, but data on its performance are lacking for histopathologically confirmed early-stage HCC.

***Purpose:*** To evaluate the sensitivity and specificity of dynamic contrast-enhanced abbreviated MRI for early-stage HCC detection, using surgical pathologic findings as the reference standard.

***Materials and Methods:*** This retrospective study was conducted at three U.S. liver transplant centers in patients with cirrhosis who underwent liver resection or transplant between January 2009 and December 2019 and standard "full" liver MRI with and without contrast enhancement within 3 months before surgery. Patients who had HCC-directed treatment before surgery were excluded. Dynamic abbreviated MRI examinations were simulated from the presurgical full MRI by selecting the coronal T2-weighted and axial three-dimensional fat-suppressed T1-weighted dynamic contrast-enhanced sequences at precontrast, late arterial, portal venous, and delayed phases. Two abdominal radiologists at each center independently interpreted the simulated abbreviated examinations with use of the Liver Imaging Reporting and Data System version 2018. Patients with any high-risk liver observations (>LR-3) were classified as positive; otherwise, they were classified as negative. With liver pathologic findings as the reference standard for the presence versus absence of early-stage HCC, the sensitivity, specificity, and their 95% CIs were calculated. Logistic regression was used to identify factors associated with correct classification.

***Results:*** A total of 161 patients with early-stage HCC (median age, 62 years [IQR, 58–67 years]; 123 men) and 138 patients without HCC (median age, 55 years [IQR, 47–63 years]; 85 men) were confirmed with surgical pathologic findings. The sensitivity and specificity of abbreviated MRI were 88.2% (142 of 161 patients) (95% CI: 83.5, 92.5) and 89.1% (123 of 138 patients) (95% CI: 84.4, 93.8), respectively. Sensitivity was lower for Child-Pugh class B or C versus Child-Pugh class A cirrhosis (64.1% vs 94.2%; $P < .001$).

***Conclusion:*** With surgical pathologic findings as the reference standard, dynamic abbreviated MRI had high sensitivity and specificity for early-stage hepatocellular carcinoma detection in patients with compensated cirrhosis but lower sensitivity in those with decompensated cirrhosis.



*Supplemental material is available for this article.*

Hepatocellular carcinoma (HCC) is a leading cause of cancer-related death worldwide and is projected to become the third leading cause of cancer death in the United States by 2035 (1,2). Curative surgical therapies provide more than 70% 5-year survival for patients with early-stage HCC, whereas patients with late-stage HCC have a median survival of only 1–2 years (3). Accordingly, the American Association for the Study of Liver Diseases and the European Association for the Study of the Liver recommend semiannual HCC surveillance in patients with cirrhosis, a major risk factor for HCC (4,5). A meta-analysis of cohort studies demonstrated that HCC surveillance improves early tumor detection and HCC-related mortality in patients with cirrhosis (6).

Practice guidelines currently recommend noncontrast liver US for HCC surveillance (4,5). However, US-based surveillance is operator-dependent (7) and has suboptimal sensitivity for early-stage HCC detection, with a meta-analysis reporting a pooled per-patient sensitivity of only 63% (8).

MRI is more sensitive than US and generally considered the best diagnostic test for HCC (9–11). However, practice guidelines have not endorsed routine use of MRI for HCC surveillance due to concerns of long in-scanner

### Abbreviations

HCC = hepatocellular carcinoma, LI-RADS = Liver Imaging Reporting and Data System


### Summary

Dynamic abbreviated MRI had high sensitivity and specificity for detecting early-stage hepatocellular carcinoma in patients with compensated cirrhosis but lower sensitivity in patients with decompensated cirrhosis.

### Key Results

- This multicenter retrospective cross-sectional study included 161 patients with cirrhosis who underwent liver MRI followed by liver resection or transplant with histopathologic confirmation of early-stage hepatocellular carcinoma (HCC) and 138 patients without HCC.
- Dynamic abbreviated MRI, comprised dynamic contrast-enhanced T1-weighted sequences, had patient-level sensitivity of 88.2% and specificity of 89.1% for detection of early-stage HCC.
- Patient-level sensitivity was lower in Child-Pugh class B or C cirrhosis than in class A (64.1% vs 94.2%; $P < .001$).


time, cost, access, and paucity of efficacy data in the surveillance setting. Prior decision analyses suggested that if the examination time and cost could be reduced by using fewer pulse sequences than standard liver MRI with and without contrast enhancement, such an abbreviated MRI could be cost-effective for HCC surveillance (12,13). This concept has led to several proposed abbreviated MRI strategies, with variations in contrast agents and pulse sequences (14,15). One of the proposed variations is the dynamic abbreviated MRI, a 6-minute screening examination using dynamic contrast-enhanced sequences, akin to multiphase contrast-enhanced CT. HCC detection with these dynamic sequences has been shown to be concordant with detection at full MRI (16,17).

Abbreviated MRI may be efficacious in HCC detection regardless of abbreviation protocol variations, with meta-analyses reporting pooled sensitivity and specificity estimates of 86% and 94%–96%, respectively (18,19). However, most studies used a composite reference standard for HCC diagnosis (ie, available histopathologic findings, imaging, and/or clinical follow-up) and may have confirmation bias and overestimation of performance. Additionally, previous studies are prone to spectrum bias, as the detection sensitivities were estimated for any stage of HCC (ie, including late-stage tumors) rather than early-stage HCC alone. The most rigorous reference standard for the presence and absence of HCC remains surgical pathologic findings. Therefore, our study aimed to evaluate the sensitivity and specificity of dynamic contrast-enhanced abbreviated MRI for early-stage HCC detection in patients with cirrhosis, with use of surgical pathologic findings as the reference standard.

## Materials and Methods

### Patients

We conducted a retrospective cross-sectional study at three U.S. academic liver transplant centers within the National Cancer Institute's Translational Liver Cancer Consortium (20). Participating sites (University of Texas Southwestern, University of Michigan, and University of Maryland) have robust multidisciplinary HCC and liver transplantation programs (20) and follow the American College of Radiology Liver Imaging Reporting and Data System (LI-RADS) for HCC imaging. From each site's surgical and medical records, we identified consecutive patients with cirrhosis who underwent surgical resection or liver transplant between January 2009 and December 2019 and abdominal MRI using extracellular gadolinium contrast material within 3 months before surgery. We excluded patients who had liver-directed therapy before surgery, did not have histopathologic confirmation of cirrhosis, or whose imaging technique deviated from the LI-RADS recommendations (eg, noncontrast, renal mass, enterography examination) or used hepatobiliary contrast enhancement. Patients with only subclinical HCCs (size, <1 cm) at histopathologic examination were also excluded, as the purpose of HCC surveillance is to detect early-stage HCC with a size of 1 cm or larger, not detect subclinical HCCs. For this study, early stage was defined per the Milan criteria: a single tumor less than 5 cm in maximum diameter or up to three tumors, all of which are less than 3 cm in maximum diameter and do not have macrovascular invasion. Patients with tumor burden beyond the Milan criteria were excluded, given that the intent of surveillance is to identify HCC at an early stage when it is amenable to curative treatment options. The patient eligibility flowchart is shown in Figure 1. The study was approved by the institutional review board at each participating site and conducted in compliance with the Health Insurance Portability and Accountability Act; the requirement for informed consent was waived.

### Abbreviated MRI and Radiologic Reporting

For each patient, the most recent presurgical liver MRI examination was selected as the index MRI examination. MRI examinations at each site included unenhanced T1-, T2-, and diffusion-weighted sequences as well as dynamic contrast-enhanced T1-weighted sequences according to LI-RADS technical recommendations (21). Dynamic contrast-enhanced imaging used an axial fat-suppressed three-dimensional T1-weighted gradient-recalled-echo sequence performed during the precontrast, late arterial, portal venous, and delayed phases following a power injection of an extracellular gadolinium-based contrast agent, as detailed in Table S1. Dynamic abbreviated MRI examination was simulated by extracting the large field of view coronal T2-weighted and dynamic T1-weighted sequences from the set of all noncontrast and contrast-enhanced sequences included in the original full MRI examination. The coronal T2-weighted sequence was also included, as technologists at the participating sites use it to prescribe axial dynamic sequences per standard clinical workflow (16). Two board-certified fellowship-trained abdominal radiologists at each site (C.H.L., with 3 years of experience, and T.Y., G.K., M.M.L., M.S.D., and B.F.L., each with 10 or more years of experience in abdominal MRI) blinded to histopathologic findings and full MRI examinations performed independent reviews of local abbreviated MRI examinations beginning in June 2020 to allow for a washout period of at least 6 months. Each reader was asked to detect high-risk liver observations (ie, LR-4, LR-5,

LR-M, and LR-TIV categories per the LI-RADS version 2018 CT/MRI algorithm) with use of only the dynamic abbreviated MRI sequences. Each reader provided the size and liver segment of each high-risk liver observation, as well a subjective assessment of examination quality (adequate, borderline, or nondiagnostic) by adopting principles of the liver visualization score of the LI-RADS Ultrasound algorithm (21,22) based on arterial phase timing, presence of artifacts, and overall image quality (Table S2).

## Data Collection

We collected demographic (age, sex, and race and ethnicity), clinical, surgical, and laboratory data from the electronic medical records. Collection of sex and race and ethnicity data was required per the funding agency. The cause of cirrhosis was classified as hepatitis C, hepatitis B, alcohol-related liver disease, nonalcoholic fatty liver disease, or other. Body mass index (calculated as patient height in meters squared divided by patient weight in kilograms) was categorized according to World Health Organization classification as follows: normal or class I, II, or III, with body mass indexes of 25, 30, 35, and 40, respectively, as cutoffs (23). Child-Pugh class was calculated to describe cirrhosis severity; Child-Pugh class A was considered compensated, and class B or C, decompensated. Surgical pathologic specimens were interpreted by the gastrointestinal pathology service of the participating sites per routine clinical care. Histopathologic findings were abstracted from templated pathology reports, including diagnosis (HCC, non-HCC malignancy, regenerative nodule, other), number of HCC nodules, maximum diameter, liver segment, presence of macrovascular invasion, and presence of cirrhosis. These features were used to confirm the early-stage HCC status as defined in the Milan criteria.

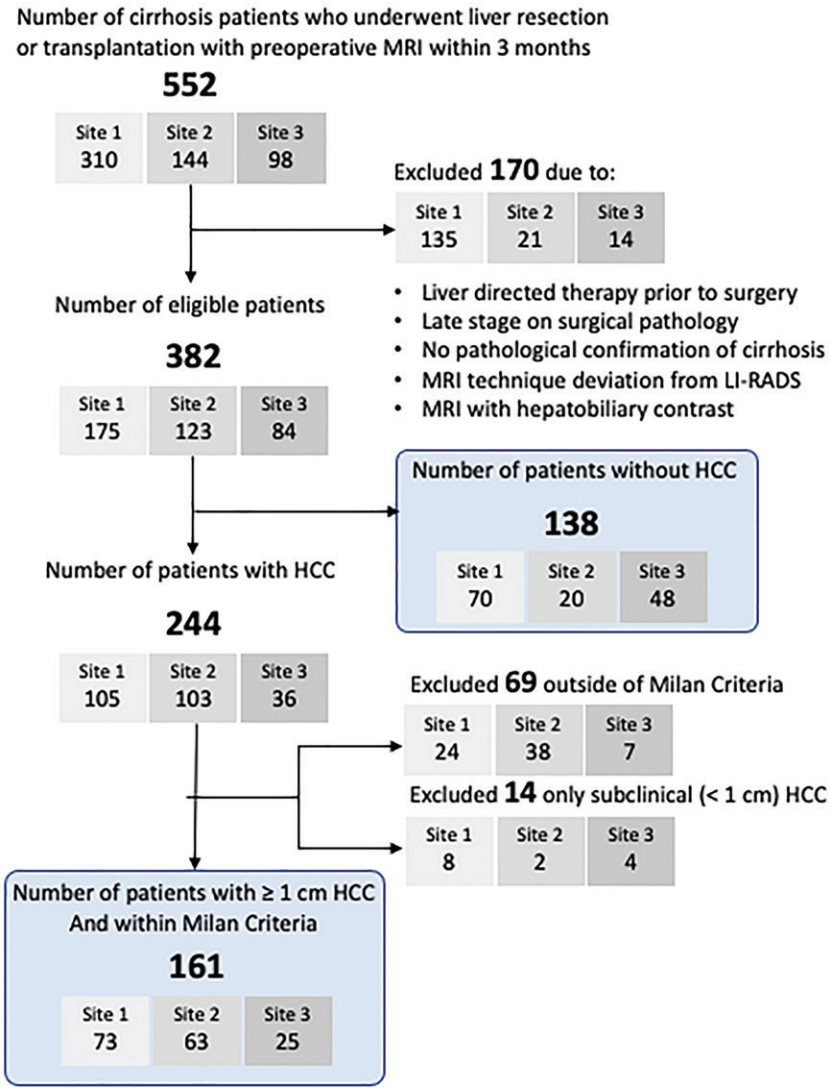


**Figure 1:** Patient eligibility flow diagram. The final study sample is indicated by rounded rectangles. HCC = hepatocellular carcinoma, LI-RADS = Liver Imaging Reporting and Data System.

## Statistical Analysis

Patient characteristics were summarized with medians and IQRs for continuous variables and with proportions for categorical variables, and differences between patient groups were tested using the Mann-Whitney *U* test or $\chi^2$ test, respectively, as appropriate. The primary outcome was per-patient sensitivity and specificity of dynamic abbreviated MRI for detecting early-stage HCC with use of surgical pathologic findings as the reference standard. A secondary outcome was per-lesion sensitivity. Sensitivity was determined among patients with surgically confirmed early-stage HCC, and specificity in those with surgically confirmed absence of HCC. All statistical analyses were performed by biostatisticians (N.M., biostatistics PhD student, under supervision of T.L.M. and Z.F., PhD-level biostatisticians with more than 10 years of experience) at an independent statistical center with use of R version 4.0.3 (The R Foundation).

For per-patient sensitivity and specificity, each abbreviated MRI examination was categorized as negative (all observations at category LR-3 or lower) or positive (any observation higher than category LR-3). This LR-3 threshold was selected a priori due to its sufficiently low positive predictive value for HCC (24,25), for which follow-up abbreviated MRI may be appropriate in a surveillance setting. This is analogous to the "subthreshold" category in LI-RADS Ultrasound, for which follow-up US at 3–6 months is recommended. Interreader agreement between radiologists regarding abbreviated MRI positivity, as well as examination quality, were calculated per site with use of the Cohen κ statistic (26). Each histologically confirmed HCC of 1 cm or larger was matched to an abbreviated MRI observation, if reported, based on size and liver segment. A size mismatch within 1 cm and location in an immediately neighboring segment (eg, segment VII vs VIII) was permitted as a match but otherwise considered a false-negative finding.

**Table 1: Characteristics of Patients with Cirrhosis with Early-Stage HCC and without HCC, Confirmed with Surgical Pathologic Findings**

| Variable | Patients without HCC (*n* = 138) | Patients with Early-Stage HCC (*n* = 161) | All Patients (*n* = 299) |
|---|---|---|---|
| Age (y)* | 55 (47–63) | 62 (58–67) | 60 (54–65) |
| Sex | | | |
| M | 85 (62) | 123 (76) | 208 (70) |
| F | 53 (38) | 38 (24) | 91 (30) |
| Race or ethnicity | | | |
| Black or African American | 17 (12) | 38 (24) | 55 (18) |
| Hispanic or Latino | 18 (13) | 16 (10) | 34 (11) |
| Non-Hispanic White | 102 (74) | 95 (59) | 197 (66) |
| Other† | 1 (1) | 12 (7) | 13 (5) |
| Body mass index*‡ | 27.6 (23.8–31.2) | 27.3 (24.1–31.1) | 27.4 (24.0–31.1) |
| Cause of liver disease | | | |
| Hepatitis C | 23 (17) | 108 (67) | 131 (44) |
| Hepatitis B | 5 (4) | 13 (8) | 18 (6) |
| Alcohol-related | 76 (55) | 32 (20) | 108 (36) |
| Nonalcoholic steatohepatitis | 53 (38) | 24 (15) | 77 (26) |
| Cryptogenic | 10 (7) | 4 (2) | 14 (5) |
| Other | 27 (20) | 10 (6) | 37 (12) |
| Ascites | | | |
| None | 13 (9) | 128 (80) | 141 (47) |
| Controlled/mild | 66 (48) | 23 (14) | 89 (30) |
| Uncontrolled/severe | 58 (42) | 6 (4) | 64 (21) |
| Unknown/not reported | 1 (1) | 4 (2) | 5 (2) |
| Encephalopathy | | | |
| None | 23 (17) | 122 (76) | 145 (49) |
| Controlled/mild | 97 (70) | 22 (14) | 119 (40) |
| Uncontrolled/severe | 15 (11) | 4 (2) | 19 (6) |
| Unknown/not reported | 3 (2) | 13 (8) | 16 (5) |
| Child-Pugh class | | | |
| A | 3 (2) | 129 (80) | 132 (44) |
| B | 29 (21) | 16 (10) | 45 (15) |
| C | 106 (77) | 16 (10) | 122 (41) |
| α-Fetoprotein level (ng/mL)* | 2.8 (2.0–4.6) | 10 (4.0–38.2) | 4.3 (2.5–14.9) |
| Number of HCCs | | | |
| None | 138 (100) | … | 138 (46) |
| 1 | … | 144 (89) | 144 (48) |
| 2 | … | 15 (9) | 15 (5) |
| 3 | … | 2 (1) | 2 (1) |
| Maximum tumor diameter (cm)* | … | 2.4 (1.8–3.5) | 2.4 (1.8–3.5) |
| Type of surgery | | | |
| Surgical resection | 2 (1) | 127 (79) | 129 (43) |
| Liver transplant | 136 (99) | 34 (21) | 170 (57) |
| Abbreviated MRI field strength | | | |
| 1.5 T | 118 (86) | 116 (72) | 234 (78) |
| 3.0 T | 20 (14) | 45 (28) | 65 (22) |
| Abbreviated MRI quality score | | | |
| A. Adequate | 61 (44) | 119 (74) | 180 (60) |
| B. Borderline | 57 (41) | 37 (23) | 94 (31) |
| C. Nondiagnostic | 20 (14) | 5 (3) | 25 (8) |

Note.—Unless otherwise specified, data are numbers of patients, with percentages in parentheses. HCC = hepatocellular carcinoma.

* Data are medians, with IQRs in parentheses.

† Other race includes American Indian or Alaskan and Native Hawaiian or other Pacific Islander.

‡ Body mass index is calculated as patient height in meters squared divided by patient weight in kilograms.

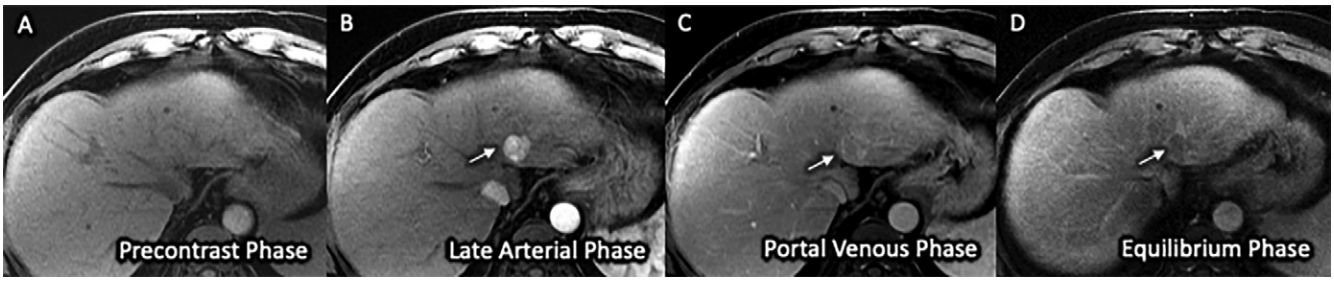


**Figure 2:** **(A–D)** Three-dimensional axial dynamic contrast-enhanced T1-weighted images (liver acquisition with volume acquisition, or LAVA) with frequency-selective fat suppression acquired on a 1.5-T GE Signa HDxt scanner in a 64-year-old man with Child-Pugh class A cirrhosis from chronic hepatitis C infection. Examination quality was rated as adequate by both readers. The images from this simulated dynamic abbreviated MRI examination demonstrate a 2.1-cm observation (arrow) in segment II with nonrim arterial phase hyper-enhancement **(A)** and delayed washout **(C)**, classified as Liver Imaging Reporting and Data System category LR-5 and confirmed as poorly differentiated hepatocellular carcinoma on the left lobectomy surgical specimen.

For per-patient pooled reader sensitivities and specificities, their respective 95% CIs were calculated using percentiles of the bootstrap distribution under patient-level resampling to account for clustering of abbreviated MRI assessments by multiple readers within a given patient. For per-lesion sensitivity, the same LR-3 threshold was applied. Although we restricted the per-patient sensitivity calculation to patients within the Milan criteria (27), we included all lesions in the per-lesion sensitivity calculation, regardless of the patient's Milan criteria status. Respective 95% CIs were calculated, again using patient-level resampling to account for clustering of multiple tumors and readers within a given patient. We examined the association of examination characteristics (eg, field strength, examination quality) and patient characteristics (eg, Child-Pugh class, cause of cirrhosis, body mass index) with abbreviated MRI sensitivity and specificity by means of subgroup analyses and univariate logistic regression with generalized estimating equations and an exchangeable working correlation matrix for multireader outcomes. Separate logistic regressions were performed for sensitivity and specificity, where the dependent variables were defined by the odds of agreement between abbreviated MRI and pathologic findings in patients with or without HCC, respectively. For each point estimate, the 95% CIs and *P* values were calculated.

An a priori power calculation demonstrated that a sample size of 139 patients with HCC and 139 without HCC was required to estimate sensitivity and specificity within a 95% CI of ±0.05, assuming these estimates to be 0.90 based on published abbreviated MRI performance data. Statistically significant difference was established either by $P < .05$ for a point estimate or its 95% confidence limit outside of the null hypothesis.

## Results

### Patient Characteristics

The patient eligibility flowchart is shown in Figure 1. In 244 patients with histopathologically confirmed HCCs, a total of 265 tumors were 1 cm or larger, 71, 140, and 54 of which were 1–1.9 cm, 2–4.9 cm, and equal to or larger than 5 cm, respectively. Sixty-nine patients were outside the Milan criteria, and 14 patients only had subclinical (<1 cm) HCCs; these patients were excluded from the patient-level analysis, as the goal of surveillance is to detect clinically actionable early-stage HCCs. Characteristics of the remaining 299 patients (161 with early-stage HCC; 138 without HCC) are presented in Table 1. The group with HCC had a median age of 62 years (IQR, 58–67 years), 123 of 161 (76%) were men, and 95 (59%) were White. The group without HCC had a median age of 55 years (IQR, 47–63 years), 85 of 138 (62%) were men, and 102 (74%) were White. Most patients with HCC had been treated with resection (127 of 161 [79%]) and were more likely to have Child-Pugh class A cirrhosis (129 of 161 [80%] vs three of 138 [2%]; $P < .001$), less likely to have ascites (29 of 161 [18%] vs 124 of 138 [90%]; $P < .001$), and less likely to have hepatic encephalopathy (26 of 161 [16%] vs 112 of 138 [81%]; $P < .001$) compared with patients without HCC, nearly all of whom had undergone liver transplant (136 of 138 [99%]). Among patients with HCC, most had unifocal tumors (144 of 161 [89%]) with a median tumor diameter of 2.4 cm (IQR, 1.8–3.5 cm). Patient characteristics per site are summarized in Table S3.

### MRI Examination Characteristics

The median time from MRI to surgery was 39 days, with an IQR of 16–66 days. Most MRI examinations were performed at 1.5 T (234 of 299 [78%]) rather than 3.0 T. The abbreviated MRI quality scores for patients with Child-Pugh class A cirrhosis differed from those with Child-Pugh class B or C cirrhosis (adequate, 108 of 132 patients [82%] vs 72 of 167 patients [43%]; borderline, 24 of 132 [18%] vs 70 of 167 [42%]; nondiagnostic, 0 of 132 [0%] vs 25 of 167 [15%]; all $P < .001$).

### Interreader Agreement

Interreader agreement for patient-level abbreviated MRI examination positivity (any observation higher than category LR-3 vs not) was moderate to strong, with Cohen κ of 0.87, 0.84, and 0.69 at sites 1, 2, and 3, respectively. Interreader agreement for examination quality categories (adequate, borderline, nondiagnostic) was only fair, with κ of 0.36, 0.28, and 0.43 at sites 1, 2, and 3, respectively.

### Abbreviated MRI Sensitivity for HCC Detection

An example of successful early HCC detection is shown in Figure 2. Patient-level sensitivity by reader ranged from 60.0% to 95.2%,

**Table 2: Patient-level Sensitivity and Specificity of Abbreviated MRI for Early-Stage HCC Detection in Patients with Cirrhosis**

| | Patients with Early-Stage HCC | | Patients without HCC | | All Patients | |
|---|---|---|---|---|---|---|
| Site and Reader | No. of Patients | Sensitivity (%) | No. of Patients | Specificity (%) | No. of Patients | Accuracy (%) |
| Site 1 | 73 | | 70 | | 143 | |
| Reader 1 | 66/73 | 90.4 (83.6, 97.3) | 59/70 | 84.3 (75.7, 92.9) | 125/143 | 87.4 (81.8, 92.3) |
| Reader 2 | 66/73 | 90.4 (83.6, 97.3) | 58/70 | 82.9 (74.3, 91.4) | 124/143 | 86.7 (81.1, 92.3) |
| Site 2 | 63 | | 20 | | 83 | |
| Reader 1 | 60/63 | 95.2 (88.9, 100) | 17/20 | 85.0 (70.0, 100) | 77/83 | 92.8 (86.7, 97.6) |
| Reader 2 | 60/63 | 95.2 (88.9, 100) | 18/20 | 90.0 (75.0, 100) | 78/83 | 94.0 (88.0, 98.8) |
| Site 3 | 25 | | 48 | | 73 | |
| Reader 1 | 17/25 | 68.0 (48.0, 84.0) | 48/48 | 100 (92.6, 100) | 65/73 | 89.0 (80.8, 95.9) |
| Reader 2 | 15/25 | 60.0 (40.0, 80.0) | 46/48 | 95.8 (89.6, 100) | 61/73 | 83.6 (75.3, 91.8) |
| Pooled estimates | 142/161 | 88.2 (83.5, 92.5) | 123/138 | 89.1 (84.4, 93.8) | 265/299 | 88.6 (85.3, 91.6) |

Note.—Data in parentheses are 95% CIs. HCC = hepatocellular carcinoma.

**Table 3: Patient-level Sensitivity and Specificity of Abbreviated MRI for Early-Stage HCC Detection across Patient Subgroups**

| | Patients with Early-Stage HCC | | | Patients without HCC | | |
|---|---|---|---|---|---|---|
| Characteristic | Sensitivity (%) | No. of Patients* | *P* Value | Specificity (%) | No. of Patients* | *P* Value |
| Age | | | | | | |
| ≤60 years | 78.7 (68.0, 87.7) | 48/61 | Reference | 90.3 (84.4, 95.2) | 84/93 | Reference |
| >60 years | 94.0 (90.0, 97.5) | 94/100 | <.001 | 86.7 (77.8, 94.4) | 39/45 | .36 |
| Sex | | | | | | |
| M | 82.9 (71.1, 93.4) | 31.5/38 | Reference | 85.8 (76.4, 94.3) | 45.5/53 | Reference |
| F | 89.8 (85.0, 94.3) | 110.5/123 | .11 | 91.2 (85.3, 95.9) | 77.5/85 | .17 |
| Body mass index[†] | | | | | | |
| <25 | 88.8 (79.6, 95.9) | 43.5/49 | Reference | 83.0 (73.4, 91.5) | 39/47 | Reference |
| ≥25 and ≤30 | 85.8 (77.6, 93.3) | 57.5/67 | .51 | 93.3 (85.6, 98.9) | 42/45 | .04 |
| >30 | 91.1 (83.3, 97.8) | 41/45 | .60 | 91.3 (82.6, 97.8) | 42/46 | .10 |
| Child-Pugh class | | | | | | |
| A | 94.2 (90.3, 97.3) | 121.5/129 | Reference | 66.7 (0, 100)[‡] | 2/3 | Reference |
| B or C | 64.1 (48.4, 79.7) | 20.5/32 | <.001 | 89.6 (84.8, 93.7) | 121/135 | .10 |
| Cause of liver disease[§] | | | | | | |
| Viral causes | 88.0 (82.5, 93.2) | 103/117 | Reference | 78.8 (63.5, 92.3) | 20.5/26 | Reference |
| Alcohol-associated | 82.1 (60.7, 100) | 11.5/14 | .38 | 94.5 (89.1, 98.4) | 60.5/64 | .003 |
| NASH | 97.2 (91.7, 100) | 17.5/18 | .13 | 100 (85.8, 100) | 24/24 | …[‖] |
| Other | 83.3 (62.5, 100) | 10/12 | .51 | 75.0 (58.3, 89.6) | 36/48 | .17 |
| Abbreviated MRI quality score | | | | | | |
| A. Adequate | 93.3 (89.1, 97.1) | 111/119 | Reference | 82.0 (73.0, 90.2) | 50/61 | Reference |
| B. Borderline | 78.4 (66.2, 90.5) | 29/37 | <.001 | 94.7 (89.5, 99.1) | 54/57 | .004 |
| C. Nondiagnostic | 40.0 (10.0, 70.0)[‡] | 2/5 | <.001 | 95.0 (85.0, 100) | 19/20 | .06 |

Note.—Data in parentheses are 95% CIs. HCC = hepatocellular carcinoma, NASH = nonalcoholic steatohepatitis.

* Number of correctly interpreted patients to the total number of patients, averaged over two readers.

[†] Body mass index is calculated as patient height in meters squared divided by patient weight in kilograms.

[‡] Estimated from $n \leq 5$ and not reliable.

[§] Hepatitis B and C categories are combined as viral causes, and the cryptogenic category is combined with "other."

[‖] For the analysis of specificity, NASH was included in the "other" category of cause of liver disease because the probability of negative abbreviated MRI results in control patients (ie, those without HCC) was 100%.

with a pooled reader sensitivity of 88.2% (142 of 161 patients) (95% CI: 83.5, 92.5) (Table 2). Sensitivity estimates across patient subgroups are detailed in Table 3. Sensitivity was lower in younger patients (78.7% vs 94.0%; $P < .001$), patients with Child-Pugh class B or C cirrhosis (64.1% vs 94.2% for class A; $P < .001$), and patients with worse abbreviated MRI quality scores (40% nondiagnostic, 78.4% borderline, 93.3% adequate; $P < .001$ for both).

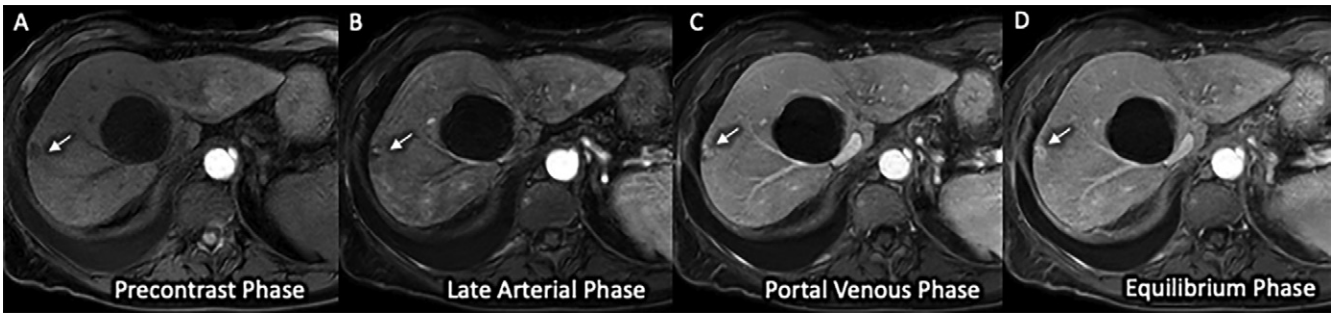


**Figure 3: (A–D)** Three-dimensional axial dynamic contrast-enhanced T1-weighted images (mDixon sequence) acquired on a 1.5-T Philips Ingenia scanner in a 66-year-old woman with Child-Pugh class C cirrhosis from alcohol use. Examination quality was rated as adequate by both readers. The images from this simulated dynamic abbreviated MRI examination demonstrate no high-risk (Liver Imaging Reporting and Data System category LR-4, LR-5, or LR-M) observation but show a T1-hypointense observation (arrow) in the periphery of segment VII, with enlarging peripheral nodular enhancement at sequential postcontrast phases consistent with hemangioma, as well as a simple cyst. These findings, including the absence of hepatocellular carcinoma, were confirmed on the liver explant specimen.

Lesion-level sensitivity by reader (Table S4]) ranged from 57.9% to 87.5%, with a pooled reader sensitivity of 79.8% (211.5 of 265 lesions) (95% CI: 75.1, 85.0). Pooled reader lesion-level sensitivity per the maximum HCC diameter was 52.8% (37.5 of 71 lesions) (95% CI: 41.2, 64.5) for tumors 1–1.9 cm, 88.6% (124 of 140 lesions) (95% CI: 84.0, 93.0) for tumors 2–4.9 cm, and 92.6% (50 of 54 lesions) (95% CI: 88.0, 97.2) for tumors equal to or larger than 5 cm. When stratified by both Child-Pugh class and HCC size (Table S5), the pooled reader sensitivity was high in Child-Pugh class A cirrhosis ($n$ = 129): 83.3%, 96.8%, and 98.1% for tumor sizes 1–1.9 cm, 2–2.9 cm, and equal to or larger than 3 cm, respectively. For Child-Pugh class B or C cirrhosis ($n$ = 32), the pooled reader sensitivity was moderate: 61.1%, 64.3%, and 71.4% for tumor sizes 1–1.9 cm, 2–2.9 cm, and equal to or larger than 3 cm, respectively.

### Abbreviated MRI Specificity

An example of successful HCC exclusion is shown in Figure 3. Patient-level specificity by reader ranged from 82.9% to 100%, with a pooled specificity of 89.1% (123 of 138 patients) (95% CI: 84.4, 93.8) (Table 2). Specificity estimates across patient subgroups of interest are detailed in Table 3. Specificity was lower in patients with viral liver disease (78.8% for viral-associated vs 94.5% for alcohol-associated disease; $P$ = .003) and patients with better abbreviated MRI quality scores (95.0% for nondiagnostic [$P$ = .06 vs adequate], 94.7% for borderline [$P$ = .004 vs adequate], and 82.0% for adequate).

## Discussion

Encouraging results for hepatocellular carcinoma (HCC) detection at abbreviated MRI have been previously reported (18,19,28), but these could have been limited by single-center samples, misclassification bias due to the lack of histopathologic confirmation, ascertainment bias due to reliance on available clinical follow-up, and spectrum bias due to the inclusion of late-stage tumors. This retrospective cross-sectional study of a multicenter sample addresses many of these limitations by using an independent histopathologic reference standard for the presence versus absence of HCC and restricting to early-stage HCCs, the intended target of screening. We found that dynamic abbreviated MRI had high patient-level detection sensitivity and specificity, both exceeding 85% when surgical pathologic findings were used as the reference standard, further supporting the potential role of abbreviated MRI for HCC surveillance. For example, the patient-level, lesion-level, and small tumor (<2 cm) sensitivities found in this study (88.2%, 79.8%, and 52.8%, respectively) in our surgical cohort are comparable with those reported in a recent meta-analysis (86%, 77%, and 69%, respectively) in true or simulated surveillance cohorts (18). The specificity of 89.1% from our study was lower than that reported in the meta-analysis (94%), potentially due to the differences in the reference standard (surgical pathologic findings vs imaging follow-up) or the cohort differences (predominantly patients with end-stage cirrhosis undergoing transplant vs a higher proportion of patients with early-stage cirrhosis undergoing surveillance). A summary of relevant previous abbreviated MRI studies and their characteristics is provided in Table S6.

Among several MRI-based strategies (14,15), dynamic abbreviated MRI has several merits. The imaging protocol can be easily replicated at most MRI facilities by using 1.5-T or 3.0-T scanners equipped with standard three-dimensional T1-weighted gradient-echo sequences. The workflow is nondisruptive, and the need for technologist education is minimal. LI-RADS interpretation of dynamic abbreviated MRI is analogous to multiphase CT interpretation and offers all LI-RADS major features needed for category LR-5 classification. For non–LR-5 observations, patients may be called back for additional unenhanced MRI examinations or referred to biopsy or follow-up imaging.

We also evaluated patient factors that could modulate the detection performance of abbreviated MRI, data for which are lacking in the literature. We did not find the sensitivity of abbreviated MRI to be modulated by obesity or by cause of cirrhosis, an important finding considering that US has worse visualization and performance in patients with obesity and those with nonviral causes of cirrhosis (29–31). Our findings therefore suggest that abbreviated MRI may serve as a viable surveillance strategy in these patients in whom US may be problematic. However, abbreviated MRI sensitivity was lower in patients with Child-Pugh class B or C cirrhosis than Child-Pugh class A cirrhosis. Site-to-site variation

in detection performance, with the lowest sensitivity at the site where the patients mostly had Child-Pugh class B or C cirrhosis and were undergoing liver transplant, appeared to be mediated by low examination quality, as patients with Child-Pugh class B or C cirrhosis had adequate quality in only 43% of examinations, compared with 82% in patients with Child-Pugh class A cirrhosis. It is possible that the liver nodularity and heterogeneity in patients with Child-Pugh class B or C cirrhosis or clinically decompensated patients (eg, due to ascites, shortness of breath) may limit all imaging-based strategies. Therefore, decision analyses are needed to determine the value and cost-effectiveness of abbreviated MRI in specific patient populations, such as those with decompensated cirrhosis.

We acknowledge several study limitations. Given our reliance on a pathologic reference standard for both HCC and lack of HCC, our patient sample does not represent a typical surveillance cohort, with most of the patients with HCC having undergone resection and having less severe liver disease. In contradistinction, the patients without HCC were primarily patients who underwent liver transplant and had more decompensated liver cirrhosis. Most patients without HCC had Child-Pugh class B or C disease and underwent transplant; only a few of them had Child-Pugh class A disease and underwent surgical resection. Therefore, it is unclear whether the specificity estimates equally apply to patients with compensated Child-Pugh class A cirrhosis. The requirement for the surgical reference standard may also introduce verification bias because concerning findings at MRI were often the impetus for surgical therapy, resulting in overestimation of abbreviated MRI sensitivity. Therefore, our findings will require further validation in consecutively enrolled surveillance cohorts.

In summary, with surgical pathologic findings as the reference standard, dynamic abbreviated MRI had high sensitivity and specificity for early-stage hepatocellular carcinoma detection, with excellent performance in compensated cirrhosis (Child-Pugh class A) but lower sensitivity in decompensated cirrhosis (Child-Pugh class B or C). If validated in prospective cohort studies, abbreviated MRI may serve as an alternative surveillance strategy in patients with compensated cirrhosis. Further research is needed to better understand causes of underperformance and potential mitigation strategies in patients with decompensated cirrhosis.

**Author contributions:** Guarantors of integrity of entire study, **T.Y., C.H.L.**; study concepts/study design or data acquisition or data analysis/interpretation, all authors; manuscript drafting or manuscript revision for important intellectual content, all authors; approval of final version of submitted manuscript, all authors; agrees to ensure any questions related to the work are appropriately resolved, all authors; literature research, **T.Y., B.F.L., M.M.L., C.H.L., K.S., A.S.L., A.G.S.**; clinical studies, **T.Y., N.D.P., B.F.L., M.M.L., C.H.L., K.S., C.T.D., T.A.J., A.A., M.S.D., P.G., N.E.R., A.S.L., A.G.S.**; experimental studies, **B.F.L., A.G.S.**; statistical analysis, **T.Y., N.M., Z.F., T.L.M.**; and manuscript editing, **T.Y., N.M., N.D.P., B.F.L., Z.F., M.M.L., G.K., T.L.M., K.S., A.A., M.S.D., P.G., N.E.R., A.S.L., A.G.S.**

**Disclosures of conflicts of interest:** **T.Y.** Research grants from Siemens Healthineers, Bayer Healthcare, Bracco, GE Healthcare, and Guerbet. **N.M.** No relevant relationships. **N.D.P.** No relevant relationships. **B.F.L.** Financial support from George Washington University. **Z.F.** Grant to institution from the National Institutes of Health. **M.M.L.** No relevant relationships. **C.H.L.** No relevant relationships. **G.K.** No relevant relationships. **T.L.M.** No relevant relationships. **K.S.** Research grants to institution from Glycotest, Hanmi Pharmaceutical, Durect Pharmaceuticals, European Foundation for the Study of Chronic Liver Failure (EF CLIF), Ocera Therapeutics, Lipocine Pharmaceuticals, and the National Cancer Institute; payment for lectures from the Scripps Clinic Liver Research Consortium. **C.T.D.** No relevant relationships. **T.A.J.** No relevant relationships. **A.A.** No relevant relationships. **M.S.D.** Royalties from Wolters Kluwer and UpToDate.com; treasurer for the Society of Advanced Body Imaging; associate editor of *Radiology*. **P.G.** No relevant relationships. **N.E.R.** Consulting fees from AstraZeneca. **A.S.L.** No relevant relationships. **A.G.S.** Grant funding from the National Institutes of Health and the Cancer Prevention and Research Institute of Texas; consulting fees from Bayer, Eisai, Genentech, AstraZeneca, Exelixis, BMS, Fujifilm Medical Sciences, Exact Sciences, Roche, Glycotest, and Grail.

## References

1. Moon AM, Singal AG, Tapper EB. Contemporary epidemiology of chronic liver disease and cirrhosis. Clin Gastroenterol Hepatol 2020;18(12):2650–2666.
2. Rahib L, Wehner MR, Matrisian LM, Nead KT. Estimated projection of US cancer incidence and death to 2040. JAMA Netw Open 2021;4(4):e214708.
3. Llovet JM, Kelley RK, Villanueva A, et al. Hepatocellular carcinoma. Nat Rev Dis Primers 2021;7(1):6.
4. Marrero JA, Kulik LM, Sirlin CB, et al. Diagnosis, staging, and management of hepatocellular carcinoma: 2018 practice guidance by the American Association for the Study of Liver Diseases. Hepatology 2018;68(2):723–750.
5. European Association for the Study of the Liver. EASL Clinical Practice Guidelines: management of hepatocellular carcinoma. J Hepatol 2018;69(1):182–236. [Published correction appears in J Hepatol 2019;70(4):817.]
6. Singal AG, Zhang E, Narasimman M, et al. HCC surveillance improves early detection, curative treatment receipt, and survival in patients with cirrhosis: a meta-analysis. J Hepatol 2022;77(1):128–139.
7. Fetzer DT, Browning T, Xi Y, Yokoo T, Singal AG. Associations of Ultrasound LI-RADS visualization score with examination, sonographer, and radiologist factors: retrospective assessment in over 10,000 examinations. AJR Am J Roentgenol 2022;218(6):1010–1020.
8. Tzartzeva K, Obi J, Rich NE, et al. Surveillance imaging and alpha fetoprotein for early detection of hepatocellular carcinoma in patients with cirrhosis: a meta-analysis. Gastroenterology 2018;154(6):1706–1718.e1.
9. Liang Y, Xu F, Guo Y, et al. Diagnostic performance of LI-RADS for MRI and CT detection of HCC: a systematic review and diagnostic meta-analysis. Eur J Radiol 2021;134:109404.
10. Colli A, Fraquelli M, Casazza G, et al. Accuracy of ultrasonography, spiral CT, magnetic resonance, and alpha-fetoprotein in diagnosing hepatocellular carcinoma: a systematic review. Am J Gastroenterol 2006;101(3):513–523.
11. Chou R, Cuevas C, Fu R, et al. Imaging techniques for the diagnosis of hepatocellular carcinoma: a systematic review and meta-analysis. Ann Intern Med 2015;162(10):697–711.
12. Goossens N, Singal AG, King LY, et al. Cost-effectiveness of risk score-stratified hepatocellular carcinoma screening in patients with cirrhosis. Clin Transl Gastroenterol 2017;8(6):e101.
13. Lima PH, Fan B, Bérubé J, et al. Cost-utility analysis of imaging for surveillance and diagnosis of hepatocellular carcinoma. AJR Am J Roentgenol 2019;213(1):17–25.
14. Brunsing RL, Fowler KJ, Yokoo T, Cunha GM, Sirlin CB, Marks RM. Alternative approach of hepatocellular carcinoma surveillance: abbreviated MRI. Hepatoma Res 2020;6:59.
15. An JY, Peña MA, Cunha GM, et al. Abbreviated MRI for hepatocellular carcinoma screening and surveillance. RadioGraphics 2020;40(7):1916–1931.
16. Khatri G, Pedrosa I, Ananthakrishnan L, et al. Abbreviated-protocol screening MRI vs. complete-protocol diagnostic MRI for detection of hepatocellular carcinoma in patients with cirrhosis: an equivalence study using LI-RADS v2018. J Magn Reson Imaging 2020;51(2):415–425.
17. Lee JY, Huo EJ, Weinstein S, et al. Evaluation of an abbreviated screening MRI protocol for patients at risk for hepatocellular carcinoma. Abdom Radiol (NY) 2018;43(7):1627–1633.
18. Gupta P, Soundararajan R, Patel A, Kumar-M P, Sharma V, Kalra N. Abbreviated MRI for hepatocellular carcinoma screening: a systematic review and meta-analysis. J Hepatol 2021;75(1):108–119.

19. Kim DH, Choi SH, Shim JH, et al. Magnetic resonance imaging for surveillance of hepatocellular carcinoma: a systematic review and meta-analysis. Diagnostics (Basel) 2021;11(9):1665.
20. Singal AG, Lok AS, Feng Z, Kanwal F, Parikh ND. Conceptual model for the hepatocellular carcinoma screening continuum: current status and research agenda. Clin Gastroenterol Hepatol 2022;20(1):9–18.
21. CT/MRI LI-RADS v2018. American College of Radiology. https://www.acr.org/Clinical-Resources/Reporting-and-Data-Systems/LI-RADS/LI-RADS-CT-MRI-v2018. Published 2018. Accessed July 4, 2021.
22. Huang DQ, Fowler KJ, Liau J, et al. Comparative efficacy of an optimal exam between ultrasound versus abbreviated MRI for HCC screening in NAFLD cirrhosis: a prospective study. Aliment Pharmacol Ther 2022;55(7):820–827.
23. Obesity: preventing and managing the global epidemic. Report of a WHO consultation. World Health Organ Tech Rep Ser 2000;894:i–xii, 1–253.
24. van der Pol CB, Lim CS, Sirlin CB, et al. Accuracy of the Liver Imaging Reporting and Data System in computed tomography and magnetic resonance image analysis of hepatocellular carcinoma or overall malignancy—a systematic review. Gastroenterology 2019;156(4):976–986.
25. Arvind A, Joshi S, Zaki T, Burkholder D, Parikh ND, Singal AG; North American Liver Cancer (NALC) Consortium. Risk of hepatocellular carcinoma in patients with indeterminate (LI-RADS 3) liver observations. Clin Gastroenterol Hepatol 2021S1542-3565(21)01307-0.
26. Landis JR, Koch GG. The measurement of observer agreement for categorical data. Biometrics 1977;33(1):159–174.
27. Mazzaferro V, Regalia E, Doci R, et al. Liver transplantation for the treatment of small hepatocellular carcinomas in patients with cirrhosis. N Engl J Med 1996;334(11):693–699.
28. Park HJ, Kim SY, Singal AG, et al. Abbreviated magnetic resonance imaging vs ultrasound for surveillance of hepatocellular carcinoma in high-risk patients. Liver Int 2022;42(9):2080–2092.
29. Chong N, Schoenberger H, Yekkaluri S, et al. Association between ultrasound quality and test performance for HCC surveillance in patients with cirrhosis: a retrospective cohort study. Aliment Pharmacol Ther 2022;55(6):683–690.
30. Schoenberger H, Chong N, Fetzer DT, et al. Dynamic changes in ultrasound quality for hepatocellular carcinoma screening in patients with cirrhosis. Clin Gastroenterol Hepatol 2022;20(7):1561–1569.e4.
31. Huang DQ, Singal AG, Kono Y, Tan DJH, El-Serag HB, Loomba R. Changing global epidemiology of liver cancer from 2010 to 2019: NASH is the fastest growing cause of liver cancer. Cell Metab 2022;34(7):969–977.e2.